Evidence on the Breakdown of the Born–Oppenheimer Approximation in the Charge Density of Crystalline ^{7}LiH/D

By Geneviève Vidal-Valat and Jean-Pierre Vidal

*Groupe de Dynamique des Phases Condensées (URA 233),
Université des Sciences et Techniques du Languedoc,
34095 Montpellier CEDEX 05, France*

and Kaarle Kurki-Suonio and Riitta Kurki-Suonio

Department of Physics, University of Helsinki, SF-00170 Helsinki, Finland

Abstract

Accurate X-ray diffraction data on LiH and LiD measured at three different temperatures are analysed in terms of multipolar radial densities searching for phenomenological indications on the nature of bonding. The average spherical charge density around the atomic positions shows typical features of an ionic crystal. The central peaks are slightly contracted compared with superimposed free ions. The Li$^+$ peak contains, however, a small but significant excess of electrons, and the H$^-$/D$^-$ peak is low and diffuse. Li$^+$ is spherical and its Debye–Waller parameters agree with the neutron diffraction values obtained by Vidal & Vidal-Valat [*Acta Cryst.* (1986), B42, 131–137]. This indicates that, within the experimental accuracy, Li$^+$ is rigid. The non-spherical multipoles are significantly stronger in the hydrogen than in the deuterium derivative. They accumulate charge along the $\langle 100 \rangle$ directions giving a phenomenological indication of 'long-distance covalency' of H–H and D–D bonding with Li$^+$ ions embedded in the middle but not contributing to the covalency. The significant deviation of the charge distribution of the anion in LiH from that in LiD indicates breakdown of the Born–Oppenheimer approximation due to coupling of the vibrations and the electronic states, which is much stronger in LiH. This is the first case – and probably the only possible – where such a breakdown can be seen by X-ray diffraction.

1. Introduction

^{7}LiH with its four electrons per molecule has the simplest electronic structure of all compounds. It has therefore been the natural first target of theoretical calculations from the early days of molecular and solid-state quantum mechanics. On the other hand, high reactivity makes it difficult from the experimental point of view and, until lately, the supporting experimental data have been scant compared with the wealth of theoretical results and predictions. For example, until 1986, the only neutron and X-ray diffraction results were those obtained by Calder, Cochran, Griffiths & Lowde (1962) in their classical work.

Recently, new interest in LiH has arisen with development of modern experimental methods and efficient computing methods. New experimental information relevant to discussion of the electronic structure of ^{7}LiH has been obtained.

Anderson & Lüty (1983) studied the isotopic effect in the Raman and phonon spectra. They stated that interpretation of the isotopic shifts as a static effect due to changes in the lattice parameter was not satisfactory indicating that some dynamical effects related to the quadratic electron–phonon coupling might be involved.

Liu (1987) studied LiH by the electron energy-loss spectrometry technique in a scanning transmission electron microscope and derived the complex dielectric constant through Kramers–Kronig transformation of the observed spectrum and discussed the charge transfer between the ions in comparison with alkaline halides. The possibility of covalency was mentioned but not considered.

Recent measurements by Loupias & Chomilier (1986), Mergy (1988) and Loupias & Garreau (1989) show large differences between the $\langle 100 \rangle$ and $\langle 110 \rangle$ directional Compton profiles indicating strong anisotropy not described in a satisfactory way by any of the known theoretical models.

Rao & Jena (1986) calculated the equilibrium lattice constant, the charge state of the ions and the electron distribution self-consistently by minimizing the total ground-state energies of several LiH clusters as a function of interatomic spacing in the Hartree–Fock approximation. They concluded that LiH is about 80% ionic in character. Rodriguez & Kunc (1987, 1989) have made a thorough study of the behaviour under pressure of the real-space distribution of the electronic charge density of lithium hydride from first principles using the density func-

tional theory, with norm-conserving pseudopotentials and Ceperley–Alder exchange. They find a strong charge transfer from lithium to hydrogen in terms of integrated densities but do not comment on the degree of ionicity. They discuss the anisotropy of the ions in terms of density contour lines but not in any integral sense. The main problem in their work seems to be the 10% error in the lattice constant. They proposed that the underlying rigid-core approximation might be a possible explanation.

A combined neutron and X-ray diffraction study of ^{7}LiH and ^{7}LiD was undertaken in view of the possibility to discuss the electronic state on the basis of the charge density. Because of the lightness of the atoms, about half of all electrons are essentially taking part in the bonding. Thus, one would expect the nature of the bonding to affect the observed charge density relatively more strongly than in any other compound – if the experimental difficulties can be overcome.

Firstly, comparison of the X-ray values of Debye–Waller parameters with their neutron values would reveal the degree of non-rigidity of the vibrating atoms. Secondly, differences between the charge densities of LiH and LiD can only occur if the electron–phonon coupling is strong enough. Thus, if observed they would yield a phenomenological measure of the violation of the Born–Oppenheimer approximation. Finally, the measurements were made at three different temperatures for both crystals in order to distinguish between dynamical and electronic effects in the charge density.

The neutron diffraction study by Vidal & Vidal-Valat (1986) was the first part of this project. The Debye–Waller factors obtained in this work could be interpreted in terms of conventional lattice dynamical models and the isotopic effects could be attributed to the difference in mass.

There seems not to exist any experimental information on the breakdown of the Born–Oppenheimer approximation in crystalline LiH. Spectroscopic studies on LiH molecules in different isotopic forms have, however, shown considerable effects.

Brieger, Renn, Sodiek & Hese (1983) reported that replacement of hydrogen by deuterium changes the shape of the interatomic potential significantly, and that electronic properties of these molecules can therefore not be properly discussed without taking the non-adiabatic effect into account. Plummer, Herbst & De Lucia (1984) concluded from their studies of low vibrational and rotational states that the Born–Oppenheimer approximation is severely violated in LiH and LiD molecules.

Chan, Harding, Stwalley & Vidal (1986) performed an extensive quantitative study of the breakdown of the Born–Oppenheimer approximation on the basis of laser-induced fluorescence spectra of the LiH isotopes combined with earlier experimental data.

They noted that changing the hydrogen isotope in the LiH molecule causes a systematic shift of the potential.

2. Experimental procedures

The single-crystal samples of ^{7}LiH and ^{7}LiD for the X-ray diffraction measurements were cut parallel to the {001} crystal faces from the same crystalline discs as the samples for the neutron diffraction study by Vidal & Vidal-Valat (1986) – synthesis of the crystals and preparation of the discs have been reported in detail in that context. The original crystal boules had been kindly provided by Dr Mathew C. Delong, University of Utah. Discs 5 mm thick and about 20 mm in diameter had been cut from the boules and submitted to a thermal and annealing treatment with subsequent quenching in order to minimize the effect of extinction on the diffraction intensities (Vidal, Vidal-Valat & Zeyen, 1985). The crystals thus obtained were colourless and optically fully transparent.

Because of the high reactivity and high hygroscopy of the crystals an efficient protection against the atmosphere was necessary. The freshly cleaved samples were sealed in Lindemann capillary tubes in anhydrous paraffin oil. This protection was seen to be perfectly transparent to the X-ray beam and it preserved the samples untouched by any atmospheric effects for at least several months.

One sample of each compound with the shape of a parallelepiped was used for the X-ray diffraction study. Relative integrated intensities of all reflexions up to 10^{10} m^{-1} in $(\sin\theta)/\lambda$ in a whole octant were collected, including 26 independent reflexions and their equivalents, on an automated four-circle Enraf–Nonius CAD-4 diffractometer with Mo $K\alpha$ radiation. The measurements were performed in the same three temperatures as the neutron diffraction measurements or at 293, 160 and 93 K for ^{7}LiH and at 293, 160 and 83 K for ^{7}LiD, three times at each temperature. The integration was done in the θ–2θ scan mode with programmed scan and aperture at the scanning speed of 2's^{-1}. The dead-time correction was automatically taken into account by the analyser.

The multiple-scattering effect was removed by setting the crystallographic and diffractometer axes differently. Moreover, the small sizes and the broad mosaic character of the thermally treated samples may further reduce any extraneous intensity effects. However, the weakness of diffracted intensities decreases the multiple-scattering effect as this effect, to be visible, requires strong intensities that can contribute by subsequent rediffraction. Renninger scans were performed on ^{7}LiH and ^{7}LiD forbidden reflexions. No effect was detected.

Basic crystallographic data on ^{7}LiH and ^{7}LiD are listed in Table 1.

Table 1. *Basic crystallographic data*

	^{7}LiH	^{7}LiD
Space group	225	225
	$Fm3m$	$Fm3m$
Sample size (mm)	$0.38 \times 0.344 \times 0.26$	$0.37 \times 0.344 \times 0.485$
Cell parameters (m)		
293 K	$a = b = c = 4.0752(7) \times 10^{-10}$	$a = b = c = 4.0615(7) \times 10^{-10}$
160 K	$a = b = c = 4.0647(7) \times 10^{-10}$	$a = b = c = 4.0516(7) \times 10^{-10}$
93 K	$a = b = c = 4.0609(7) \times 10^{-10}$	
83 K		$a = b = c = 4.0447(7) \times 10^{-10}$
	$\alpha = \beta = \gamma = 90°$	
Atomic positions	Li$^+$: 0 0 0	Li$^+$: 0 0 0
	H$^-$: $\frac{1}{2}$ 0 0	D$^-$: $\frac{1}{2}$ 0 0
Site symmetry	$m3m$	$m3m$
Matrix of local coordinate axes	Li$^+$	H$^-$ or D$^-$
	$\begin{bmatrix} 1 & 0 & 0 \\ 0 & 1 & 0 \\ 0 & 0 & 1 \end{bmatrix}$	$\begin{bmatrix} 1 & 0 & 0 \\ 0 & 1 & 0 \\ 0 & 0 & 1 \end{bmatrix}$
Site-symmetric harmonics (Kara & Kurki-Suonio, 1981)	O_e	O_e
Atomic scattering factors *International Tables for X-ray Crystallography* (1974)	Li$^+$	
Open configuration of Hurst (1959)	H$^-$	D$^-$
Linear absorption coefficient (mm^{-1})	0.017	0.022

3. Refinement of the reference model

In order to analyse the crystal charge density in terms of atomic multipole expansions a preliminary theoretical model is required. In principle, the analysis is based on the conventional rigid-core assumption and the elementary model consisting of rigid ions in harmonic motion, based on suitable theoretical atomic scattering factors, is sufficient. The only parameters to be refined are, in the present case, just the isotropic Debye–Waller factors of each ion. The rigid-core assumption then implies, according to the general reciprocity argument, that the charge densities at the atomic centres and the structure factors at large $(\sin \theta)/\lambda$ are well represented by the model.

This yields two different criteria for evaluation of the parameters. Correspondingly, one can use two different methods, the Fourier method fitting the charge densities at nuclear positions or the least-squares method fitting the structure factors or intensities of high-order reflexions. The Fourier method has the advantage of using the whole set of experimental structure factors while the least-squares fitting must, by the nature of the criterion, be restricted to the use of high-order data only. Any additional experimental parameters like the scale factor and the extinction parameters complicate the situation.

It is possible to include the scale factor in the Fourier refinement and it is, in fact, included in our refinement program referred to as the iterative procedure (Vidal & Vidal-Valat, 1986), while the possibility to include any extinction parameters has not been studied. The potential presence of significant extinction therefore makes the use of least-squares fitting necessary – we use the *LINEX* program by Becker & Coppens (1975). Restriction to high-order data, however, increases strongly the correlations of these parameters with the Debye–Waller factors and with

the scale factors and, hence, discussion of extinction requires some compromise between a high-order refinement, leading to wide mathematical indeterminacy of the parameters, and an all-data refinement, where true deviations from the model are artificially minimized and the resulting values, thus, distorted.

For Li$^+$ the relativistic Hartree–Fock values of *International Tables for X-ray Crystallography* (1974) are used. For H$^-$ (and D$^-$) several different atomic factors were tried. [Both H and H$^-$ from the *International Tables for X-ray Crystallography*, both the radially corrected and the uncorrected H$^-$ of Hurst, Miller & Matsen (1958), both the closed-configuration and the open-configuration crystal-field values for H$^-$ of Hurst (1959).] Clearly, the open-configuration crystal-field values of Hurst yielded the best overall fit for all data and they were therefore adopted as the basis of the reference model.

There was no indication of significant extinction effects in the data. None of the extinction models combined with any of the theoretical values led to significant improvement of the fit. Therefore no extinction parameters were used in the refinement of the model and both methods could be used and compared with each other.

This is the stage where comparison with the neutron diffraction results is relevant. It is commonly thought in the context of the rigid-core assumption that it is the nucleus which determines the centre of the rigid core and, thus, the core and the nucleus move together with the same amplitude. If this is true, the Debye–Waller factors as determined from the X-ray and neutron measurements should have equal values.

This is certainly a good assumption for atoms possessing a core formed by the closed inner shells and some outer electrons as a screen against the surroundings. Even then it can be argued that the changes of the outer-electron wave functions along

with the vibrations of the atom have a time-dependent effect on the core wave functions, in the first place through the orthogonality requirement due to the identity of electrons (or Pauli exclusion principle). This effect would both violate the rigidity of the core and decouple the nuclear motion from the core motion. Qualitatively, the direction of this effect would be such that the nucleus would have larger amplitude than the core, and in any case a momentary dipole moment would arise, which would have a dynamical effect on the outer-electron wave functions. The first mechanism works also within the Born–Oppenheimer approximation while the second does not.

In the present case none of the ions consists of a core plus outer electrons. The Li^+ cation is, however, still a rather compact entity and it seems reasonable to consider it to be approximately rigid, at least compared to the diffuse H^- or D^- anion. Its electrons form a $1s^2$ core which, according to Grosso, Pastori Paravicini & Resta (1976) suffers only negligible deformation when the LiH crystal is formed. Correspondingly, for Li^+ the X-ray Debye–Waller factor should have a better defined physical meaning while for the hydrogen (deuterium) it is only descriptive representing the dynamical averaging of the charge density around the centre.

From these considerations it must be concluded that the neutron values as such cannot be assumed to be correct for the reference model of the charge density analysis, but that the error for lithium would be much smaller than for hydrogen/deuterium. Rather, it would be interesting to note whether the X-ray values deviate significantly from the neutron values and how large the deviation is as a semiquantitative overall measure of the coupling between the electronic state and the lattice vibrations as described above. Moreover, differences between LiH and LiD in this respect are important. Primarily, they differ in lattice dynamics only due to the different masses of H and D but not in their electronic states as determined by the Coulomb interactions in the Born–Oppenheimer approximation – as far as the magnetic interaction with the nuclei can be neglected. Thus, such differences would reflect the degree of violation of the Born–Oppenheimer approximation.

In order to discuss these effects the Debye–Waller factors B_{Li} and B_H or B_D were refined together with the scale factor k in the following different ways:

1. Least-squares fit of high-order data (*LINEX*) (1s ho in Table 2):

    (*a*) with all three parameters varied independently;

    (*b*) with B_{Li} fixed at the neutron value.

2. Charge-density fit at atomic centres (Fourier in Table 2):

    (*a*) giving both ions equal weight in the scale refinement (1; 1);

    (*b*) fitting the scale on the basis of Li^+ alone (1; 0).

The resulting B expressed in $10^{-20}\ m^2$ and k are given in Table 2 together with the neutron values for which the two methods lead to numerical equal results. [In the 'iterative method' weights (0.4; 1) and (0.6; 1) have been used in the scale refinement for Li and H and Li and D, respectively, corresponding to the accuracies of the scattering lengths, *cf.* Vidal & Vidal-Valat, 1986.)

The scale factors k listed in Table 2 are ratios of structure factors as obtained in different refinements. The variations of scale obtained by different refinements are less than ±1% for LiD and, thus, insignificant, while for LiH they range up to ±3%. This already suggests some real differences in the electronic nature of H^- and D^- data, the latter leading also to clearly better fits in terms of structure factors. It can be noted that independently of the method of refinement B_{Li} has an obvious unique dependence on the scale factor. This indicates that for lithium the two methods of refinement are equivalent as they were in the refinement of neutron data and that the two criteria are essentially different when applied to the anion. This can be understood on the basis of the diffuse nature of the anion which makes an overall refinement clearly different from the peak-only refinement. This is even more obvious in the all-data least-squares refinement – not recorded in the table – yielding B_{Li} still reasonably close to the values

Table 2. *Refinement of parameters*

LiH

	Neutron		X-ray			
	1s	Fourier (0.4; 1)	1s ho (1a)	1s ho Li fixed (1b)	Fourier (1; 1) (2a)	Fourier (1; 0) (2b)
293 K						
B_{Li}	1.191 (16)	1.195	1.182 (16)	1.195	1.248	1.207
B_H	1.711 (16)	1.715	1.773 (160)	1.822 (115)	1.592	1.503
k			1.0147	1.0062	0.9780	1
160 K						
B_{Li}	0.766 (24)	0.762	0.767 (6)	0.762	0.845	0.810
B_H	1.553 (34)	1.550	1.537 (80)	1.515 (70)	1.473	1.386
k			1.0288	1.0324	0.9800	1
93 K						
B_{Li}	0.640 (8)	0.644	0.645 (16)	0.644	0.715	0.683
B_H	1.485 (16)	1.483	1.473 (160)	1.465 (142)	1.347	1.268
k			1.0242	1.0255	0.9820	1

LiD

	Neutron		X-ray			
	1s	Fourier (0.6; 1)	1s ho (1a)	1s ho Li fixed (1b)	Fourier (1; 1) (2a)	Fourier (1; 0) (2b)
293 K						
B_{Li}	1.048 (16)	1.046	1.044 (8)	1.046	1.071	1.060
B_D	1.449 (16)	1.448	1.482 (160)	1.493 (95)	1.382	1.357
k			1.0082	1.0073	0.9938	1
160 K						
B_{Li}	0.684 (11)	0.688	0.689 (8)	0.688	0.712	0.703
B_D	1.188 (10)	1.189	1.193 (80)	1.201 (75)	1.097	1.076
k			1.0086	1.0087	0.9948	1
83 K						
B_{Li}	0.591 (8)	0.593	0.603 (4)	0.593	0.610	0.602
B_D	1.100 (8)	1.101	1.061 (55)	1.023 (49)	1.056	1.038
k			0.9980	1.0047	0.9955	1

obtained above, but completely different B_H and B_D with very large limits of error, particularly in the case of LiH.

In view of the clear-cut dependence of B_{Li} on the scale factor it can be noted that its deviations from the neutron values are not significant, the scale factors of column (1b) express uniquely the change of scale from the adopted values required to make the X-ray values equal to the neutron values. It can therefore not be stated on the basis of this comparison whether they really are equal, slightly larger or slightly smaller.

It is, however, concluded that the differences in anion Debye–Waller factor reflect some real phenomenon which is stronger for LiH than LiD. The values (2b) were adopted for the reference model used in the charge density analysis. Table 3 gives the experimental structure factors F_o, the theoretical structure factors F_c and the experimental uncertainties δF_o.

4. The course of analysis

Once the reference model has been fixed the course of the calculations required for the multipole analysis of atomic charge densities is straightforward. The principles of the analysis have been presented previously in different contexts (Vidal-Valat, Vidal & Kurki-Suonio, 1978; Vidal, Vidal-Valat, Galtier & Kurki-Suonio, 1981; Kurki-Suonio & Sälke, 1984, 1986).

First the average radial charge density $4\pi r^2 \rho_0(r)$ and the corresponding radial electron count $Z_0(r) = \int_0^r 4\pi r^2 \rho_0(r) \, dr$ of each ion are calculated. Here Gaussian representation $\sum a_i \exp[-b_i (\sin^2 \theta)/\lambda^2]$ of the theoretical atomic factors is used to account for the residual term (Sälke & Kurki-Suonio, 1984). The results for the room temperature are shown in Figs. 1(a) to (d). The results for the low temperatures differ slightly. The differences can be characterized by parameters listed in Table 4. The radii r are given in 10^{-10} m, the radial densities in $e \times 10^{10}$ m^{-1} and the electron counts in e.

On the basis of the spherical behaviour the radii 0.90×10^{-10} and 1.30×10^{-10} m are used to calculate the multipolar radial atomic factors for Li$^+$ and H$^-$ or D$^-$, respectively. The calculation involved all components up to tenth order. Figs. 2(a), (b), (c) show the significant ones with their experimental error bars. In Li$^+$ the only significant component is fourth order in LiH. From the behaviour of the corresponding radial density, Fig. 3, it is, however, concluded that this is not a genuine feature of the charge density of Li$^+$ but reflects only the strong overlapping of the diffuse anion. In hydrogen all components up to eighth order are significant, but the radius is not sufficiently large to yield them in their full strength.

Therefore, the spherical component Δf_0 is added to the theoretical atomic factor of Li$^+$ and the result is used to subtract the lithium contribution from the experimental structure factors given in Table 3 as $F_o(H^-)$ and $F_o(D^-)$. This yields experimental structure factors for the virtual H$^-$ or D$^-$ lattice. On the basis of these prepared data the average radial charge density and electron count are calculated for the H$^-$ or D$^-$ ion as in the first stage, see Fig. 4 and Table 4.

The radial multipolar scattering factors can now be calculated for the H$^-$ or D$^-$ ion using spherical partitioning with larger radii. Three different radii, 1.40×10^{-10}, 1.50×10^{-10} and 1.60×10^{-10} m were used to discuss the significance of the different multipole orders. Figs. 5(a), (b) show these results for the largest radius, which, according to Table 4, corresponds to the total of two electrons.

The different multipole components are represented also in real space in terms of radial densities $B_n r^2 \rho_n(r)$, Fig. 3 for Li$^+$ and Figs. 6(a), (b) for H$^-$ and D$^-$ in the anion-only lattices. The normalization constants $B_n = \int_{K_n < 0} K_n(\theta, \varphi) \, d\Omega$ ($B_0 = 4\pi$, $B_4 = 2.30$, $B_6 = 2.22$, $B_8 = 1.78$) are determined so that the corresponding radial electron count $Z_n(r) = B_n \int_0^r r^2 \rho_n(r) \, dr$ represents the number of electrons participating in the angular rearrangements in the component. The numbers under the lobes of the curves are electron counts corresponding to the marked areas under the curves. They are given separately for the three temperatures in order to discuss the possible dependence on temperature.

Finally, the results are visualized in terms of conventional difference density maps. Fig. 7 shows difference Fourier maps of the anion-only lattice at the three temperatures in the [110]–[001] plane with the anion site at the centre. Fig. 8 shows multipolar maps of the difference density resulting from the significant multipole components of H$^-$. Figs. 9 and 10 are the corresponding maps for D$^-$. Attention should be paid to the density interval of the contours which in the LiD maps is only half of that of the LiH maps.

5. Discussion of results

Spherical behaviour

From the spherical density, Figs. 1(a), (c), Table 4, it is evident that lithium occurs in these crystals as a compact Li$^+$ ion with two electrons. It is moderately well separable from its crystalline environment. A well defined minimum of radial density defines its radius of best separation. However, the value at minimum is relatively high compared with cations in other ionic crystals and the electron count within this radius is about 0.14e in excess of the ideal value, indicating strong overlap with the very diffuse anion.

The reduction of the radial density in the overlap region in comparison with the reference model is typical of ionic crystals and improves the separability of Li$^+$. This feature is stronger in LiH than in LiD.

Table 3. *Experimental and theoretical structure factors for* LiH *and* LiD *at different temperatures*

LiH (293 K) / **LiD (293 K)**

h	k	l	2(sin θ)/λ (Å⁻¹)	F_o	F_c	$F_o(H^-)$	δF_o	h	k	l	2(sin θ)/λ (Å⁻¹)	F_o	F_c	$F_o(D^-)$	δF_o
0	0	0	0.0000	16.0000	16.0000	7.93916		0	0	0	0.0000	16.0000	16.0000	7.94896	
1	1	1	0.4250	4.0588	4.2880	-2.55752	0.02400	1	1	1	0.4265	4.2882	4.3224	-2.35387	0.02120
2	0	0	0.4908	8.2616	7.8913	2.05147	0.00800	2	0	0	0.4924	8.0413	7.9388	1.79581	0.00400
2	2	0	0.6941	5.7298	5.5685	0.85906	0.01680	2	2	0	0.6964	5.7133	5.6457	0.77773	0.03400
3	1	1	0.8139	3.6458	3.6493	-0.45283	0.02880	3	1	1	0.8166	3.7229	3.7275	-0.45543	0.02600
2	2	2	0.8500	4.1695	4.2479	0.29371	0.00080	2	2	2	0.8529	4.3396	4.3407	0.38026	0.02200
4	0	0	0.9815	3.4444	3.3516	0.32227	0.02040	4	0	0	0.9849	3.4851	3.4519	0.26845	0.00080
3	3	1	1.0696	2.4665	2.5193	-0.20713	0.01200	3	3	1	1.0732	2.6080	2.6125	-0.16469	0.01840
4	2	0	1.0974	2.6804	2.6968	0.13830	0.00280	4	2	0	1.1011	2.7886	2.7995	0.14651	0.00120
4	2	2	1.2021	2.1712	2.1999	0.08147	0.00440	4	2	2	1.2062	2.2781	2.3020	0.08687	0.00680
3	3	3	1.2751	1.7330	1.7522	-0.08140	0.01040	3	3	3	1.2794	1.8160	1.8458	-0.09901	0.00880
5	1	1	1.2751	1.7275	1.7522	-0.08690	0.01000	5	1	1	1.2794	1.8101	1.8458	-0.10495	0.00360
4	4	0	1.3881	1.4982	1.5089	0.05037	0.00720	4	4	0	1.3928	1.5950	1.6045	0.05042	0.01120
5	3	1	1.4517	1.2489	1.2418	-0.02235	0.00240	5	3	1	1.4566	1.3357	1.3291	-0.02882	0.00280
4	4	2	1.4723	1.2592	1.2644	0.04089	0.00760	4	4	2	1.4773	1.3523	1.3555	0.04188	0.00080
6	0	0	1.4723	1.2503	1.2644	0.03199	0.00880	6	0	0	1.4773	1.3582	1.3555	0.04781	0.00400
6	2	0	1.5520	1.0655	1.0662	0.03394	0.00160	6	2	0	1.5572	1.1473	1.1523	0.02902	0.00320
5	3	3	1.6091	0.8970	0.8956	-0.01689	0.00520	5	3	3	1.6145	0.9722	0.9741	-0.02411	0.00280
6	2	2	1.6277	0.9094	0.9039	0.03110	0.00360	6	2	2	1.6332	0.9927	0.9848	0.03346	0.00680
4	4	4	1.7001	0.7641	0.7699	0.01260	0.00360	4	4	4	1.7058	0.8425	0.8457	0.01589	0.00400
7	1	1	1.7524	0.6646	0.6557	-0.00583	0.00320	7	1	1	1.7583	0.7360	0.7250	-0.00524	0.00240
5	5	1	1.7524	0.6607	0.6557	-0.00973	0.00320	5	5	1	1.7583	0.7297	0.7250	-0.01158	0.00360
6	4	0	1.7695	0.6607	0.6584	0.01499	0.00320	6	4	0	1.7755	0.7315	0.7292	0.01634	0.00280
6	4	2	1.8363	0.5658	0.5652	0.00898	0.00280	6	4	2	1.8425	0.6330	0.6311	0.01211	0.00360
5	5	3	1.8848	0.4843	0.4865	-0.01499	0.00240	5	5	3	1.8912	0.5439	0.5467	-0.01568	0.00360
7	3	1	1.8848	0.4949	0.4865	-0.00439	0.00240	7	3	1	1.8912	0.5500	0.5467	-0.00954	0.00400
8	0	0	1.9631	0.4280	0.4205	0.01036	0.00200	8	0	0	1.9697	0.4837	0.4773	0.01163	0.00360

LiH (160 K) / **LiD (160 K)**

h	k	l	2(sin θ)/λ (Å⁻¹)	F_o	F_c	$F_o(H^-)$	δF_o	h	k	l	2(sin θ)/λ (Å⁻¹)	F_o	F_c	$F_o(D^-)$	δF_o
0	0	0	0.0000	16.0000	16.0000	7.97036		0	0	0	0.0000	16.0000	16.0000	7.95592	
1	1	1	0.4261	4.1756	4.3996	-2.54102	0.01240	1	1	1	0.4275	4.3689	4.4056	-2.37219	0.02640
2	0	0	0.4920	8.3870	8.0361	2.04311	0.03320	2	0	0	0.4936	8.1853	8.0888	1.81344	0.02040
2	2	0	0.6958	5.9380	5.8000	0.83795	0.02920	2	2	0	0.6981	5.9344	5.8732	0.79184	0.01160
3	1	1	0.8160	3.9126	3.9103	-0.45787	0.00400	3	1	1	0.8186	3.9572	3.9542	-0.46602	0.00400
2	2	2	0.8522	4.4478	4.5281	0.29009	0.01200	2	2	2	0.8550	4.6041	4.6114	0.39049	0.00920
4	0	0	0.9841	3.7482	3.6568	0.31853	0.01840	4	0	0	0.9873	3.7854	3.7452	0.28869	0.00080
3	3	1	1.0724	2.7913	2.8254	-0.19765	0.01360	3	3	1	1.0776	2.8830	2.8890	-0.17953	0.00160
4	2	0	1.1002	3.0080	3.0118	0.14955	0.00600	4	2	0	1.1038	3.0848	3.1022	0.15100	0.00160
4	2	2	1.2052	2.5097	2.5152	0.10525	0.00480	4	2	2	1.2091	2.5860	2.6054	0.10062	0.00120
3	3	3	1.2784	2.0275	2.0579	-0.09629	0.01000	3	3	3	1.2825	2.1042	2.1287	-0.10284	0.00120
5	1	1	1.2784	2.0255	2.0579	-0.09822	0.00600	5	1	1	1.2825	2.0984	2.1287	-0.10867	0.01440
4	4	0	1.3917	1.7885	1.8081	0.04494	0.00880	4	4	0	1.3962	1.8876	1.8946	0.05975	0.00920
5	3	1	1.4555	1.5247	1.5278	-0.03238	0.00440	5	3	1	1.4602	1.6048	1.5989	-0.03582	0.00080
4	4	2	1.4761	1.5377	1.5511	0.03696	0.01360	4	4	2	1.4809	1.6240	1.6348	0.04021	0.00320
6	0	0	1.4761	1.5407	1.5511	0.03990	0.00760	6	0	0	1.4809	1.6227	1.6348	0.03890	0.00800
6	2	0	1.5560	1.3265	1.3390	0.02658	0.00240	6	2	0	1.5610	1.4242	1.4196	0.04385	0.00280
5	3	3	1.6133	1.1505	1.1546	-0.02094	0.00400	5	3	3	1.6185	1.2238	1.2226	-0.02554	0.00120
6	2	2	1.6319	1.1656	1.1622	0.03333	0.00800	6	2	2	1.6372	1.2444	1.2394	0.03520	0.00240
4	4	4	1.7045	1.0128	1.0134	0.02164	0.00480	4	4	4	1.7100	1.0913	1.0871	0.02731	0.00520
7	1	1	1.7569	0.8881	0.8860	-0.00642	0.00440	7	1	1	1.7626	0.9542	0.9494	-0.01495	0.00480
5	5	1	1.7569	0.8932	0.8860	-0.01148	0.00520	5	5	1	1.7626	0.9526	0.9494	-0.01646	0.00280
6	4	0	1.7741	0.8889	0.8873	0.01751	0.00680	6	4	0	1.7798	0.9556	0.9575	0.01573	0.00280
6	4	2	1.8410	0.7825	0.7797	0.01354	0.00400	6	4	2	1.8470	0.8513	0.8465	0.01824	0.00320
5	5	3	1.8897	0.6984	0.6889	-0.00323	0.00360	5	5	3	1.8958	0.7481	0.7471	-0.01450	0.00360
7	3	1	1.8897	0.7006	0.6889	-0.00110	0.00360	7	3	1	1.8958	0.7490	0.7471	-0.01360	0.00360
8	0	0	1.9682	0.6152	0.6080	0.01083	0.00320	8	0	0	1.9745	0.6706	0.6680	0.01027	0.00480

LiH (93 K) / **LiD (83 K)**

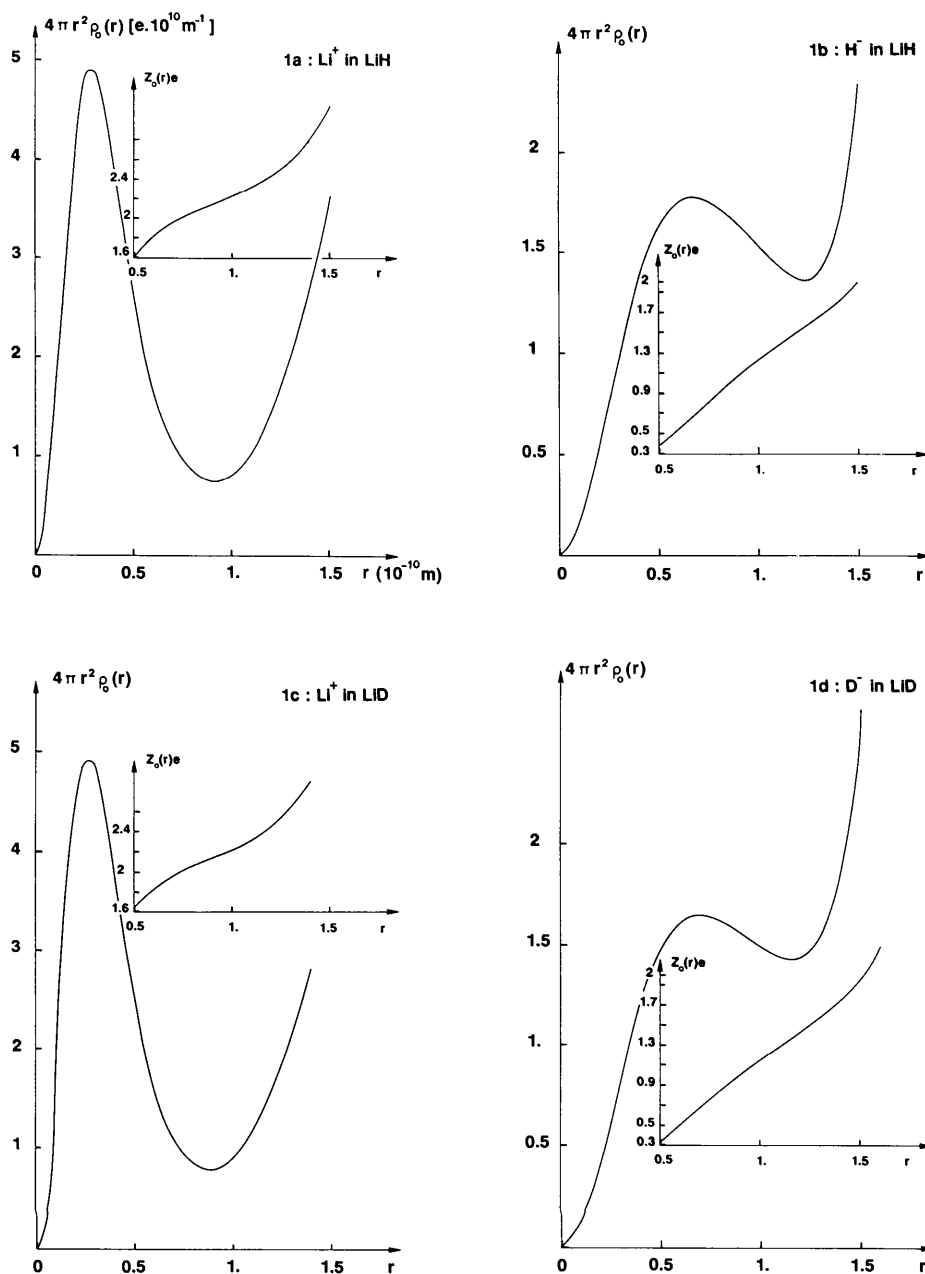| h	k	l	2(sin θ)/λ (Å⁻¹)	F_o	F_c	$F_o(H^-)$	δF_o	h	k	l	2(sin θ)/λ (Å⁻¹)	F_o	F_c	$F_o(D^-)$	δF_o
0	0	0	0.0000	16.0000	16.0000	7.96324		0	0	0	0.0000	16.0000	16.0000	7.97412	
1	1	1	0.4265	4.2093	4.4277	-2.54786	0.00400	1	1	1	0.4282	4.3929	4.4358	-2.36172	0.02200
2	0	0	0.4925	8.4351	8.0910	2.04205	0.02920	2	0	0	0.4945	8.2093	8.1211	1.81518	0.02080
2	2	0	0.6965	6.0193	5.8829	0.84387	0.00600	2	2	0	0.6993	5.9714	5.9295	0.77929	0.02960
3	1	1	0.8167	4.0033	3.9911	-0.45529	0.00800	3	1	1	0.8200	4.0183	4.0211	-0.46868	0.01600
2	2	2	0.8530	4.5499	4.6269	0.30076	0.00400	2	2	2	0.8564	4.6686	4.6822	0.38731	0.00440
4	0	0	0.9850	3.8350	3.7645	0.30459	0.01200	4	0	0	0.9889	3.8574	3.8246	0.28155	0.00080
3	3	1	1.0734	2.8955	2.9264	-0.19823	0.00560	3	3	1	1.0777	2.9708	2.9706	-0.17630	0.01480
4	2	0	1.1013	3.1148	3.1237	0.15057	0.00160	4	2	0	1.1057	3.1652	3.1863	0.14553	0.00640
4	2	2	1.2064	2.6167	2.6281	0.10440	0.01280	4	2	2	1.2112	2.6883	2.6916	0.11388	0.00520
3	3	3	1.2796	2.1300	2.1634	-0.10167	0.01040	3	3	3	1.2847	2.2002	2.2139	-0.09659	0.01760
5	1	1	1.2796	2.1199	2.1634	-0.11180	0.00640	5	1	1	1.2847	2.1940	2.2139	-0.10281	0.00640
4	4	0	1.3930	1.8937	1.9177	0.04386	0.00200	4	4	0	1.3986	1.9808	1.9803	0.06422	0.00760
5	3	1	1.4568	1.6263	1.6302	-0.03537	0.00080	5	3	1	1.4627	1.6822	1.6823	-0.04556	0.00320
4	4	2	1.4775	1.6622	1.6576	0.05795	0.01320	4	4	2	1.4834	1.7243	1.7189	0.05407	0.00080
6	0	0	1.4775	1.6502	1.6576	0.04560	0.00800	6	0	0	1.4834	1.7231	1.7189	0.05287	0.00840
6	2	0	1.5574	1.4356	1.4417	0.03507	0.00160	6	2	0	1.5637	1.5013	1.5014	0.03752	0.00080
5	3	3	1.6148	1.2522	1.2505	-0.01716	0.00600	5	3	3	1.6212	1.3021	1.3014	-0.02804	0.00640
6	2	2	1.6334	1.2486	1.2607	0.01932	0.00320	6	2	2	1.6400	1.3162	1.3185	0.02703	0.00520
4	4	4	1.7061	1.0973	1.1076	0.01310	0.00560	4	4	4	1.7129	1.1702	1.1634	0.02990	0.00560
7	1	1	1.7586	0.9884	0.9741	-0.00120	0.00480	7	1	1	1.7656	1.0239	1.0225	-0.01880	0.00520
5	5	1	1.7586	0.9844	0.9741	-0.00515	0.00560	5	5	1	1.7656	1.0299	1.0225	-0.01278	0.00520
6	4	0	1.7757	0.9766	0.9771	0.01627	0.00240	6	4	0	1.7828	1.0305	1.0307	0.01800	0.00200
6	4	2	1.8428	0.8702	0.8652	0.01649	0.00520	6	4	2	1.8501	0.9162	0.9166	0.01407	0.00280
5	5	3	1.8915	0.7818	0.7689	-0.00140	0.00400	5	5	3	1.8991	0.8162	0.8142	-0.01286	0.00560
7	3	1	1.8915	0.7720	0.7689	-0.01122	0.00520	7	3	1	1.8991	0.8154	0.8142	-0.01366	0.00320
8	0	0	1.9700	0.7021	0.6849	0.02145	0.00360	8	0	0	1.9779	0.7306	0.7320	0.00767	0.00360

Fig. 1. Radial charge densities around the atomic positions in LiH and LiD.

As a consequence, the radial density at the minimum is slightly lower in LiH while the radius of the minimum is larger. Otherwise, the spherical behaviour of the Li^+ charge distribution in LiH does not differ from that of LiD. At the lower temperatures, the radius and the minimum radial density are slightly smaller, understandably due to the smaller amplitudes of vibration.

The nature of the anion radial density, Figs. 1(b), (d), Table 4, is different. The central peak is low and the limiting minimum is broad and shallow. The deviations of the deuterium charge distribution from the reference model are very small. The radius of the best separation, the minimum radial density and the electron count at the minimum remain unchanged. In the case of hydrogen, on the contrary, the experimental charge density at the overlap area is significantly lower than in the model. As a result, the radius of best separation is larger by about 0.1×10^{-10} m, and the corresponding electron count is larger. Still, even the largest of the electron counts is only 1.6e. The anion is so diffuse that an essential part of its electron distribution extends to larger distances. This makes necessary the subtraction of the cation before the nature of the anion can be properly discussed.

In the anion-only lattices, Fig. 4, Table 4, the radii of best separation are significantly larger, but the corresponding electron counts are still low. It can be noted that these radii are clearly smaller than half the distance between neighbouring anions (1.44×10^{-10} m). This can probably be interpreted as an indication of bonding charge density and, hence, of some covalency of the anion lattice. The study of non-spherical multipoles will give more light to this question.

Non-spherical components

From the radial scattering factors corresponding to the cubic harmonics, Figs. 2(a), (b), (c), it is concluded that there is within the SVP (spherical volume partitioning) sphere a small but significant fourth-order component in Li^+ of LiH but not in LiD, all other non-spherical components being zero well below the limits of accuracy. However, the corresponding radial density, Fig. 3, does not allow one to interpret this as a feature of Li^+. It increases monotonously and thus joins naturally to the rising contribution of the neighbours.

Fig. 5(a) for H^- and Fig. 5(b) for D^- shows that the anions are significantly deformed, H^- much more strongly than D^-. The deformations are not consistent with a simple low-order multipolar behaviour. The components 4, 6 and 8 have clearly equal significance and only the tenth remains unimportant within the SVP radius. The corresponding radial densities, Figs. 6(a), (b), indicate that they represent angular re-

Table 4. *Spherical characteristics of the ions*

T	r_{max}	$4\pi r^2 \rho_0$	r_{min}	$4\pi r^2 \rho_0$	Z_0	r_{2e}
Li^+ in ^{7}LiH						
293 K	0.29	4.915	0.92	0.741	2.14	0.74
160 K	0.26	5.080	0.90	0.688	2.14	0.72
93 K	0.25	5.180	0.89	0.674	2.14	0.72
H^- in ^{7}LiH						
293 K	0.68	1.771	1.24	1.365	1.58	1.50
160 K	0.70	1.750	1.24	1.347	1.56	1.51
93 K	0.69	1.752	1.26	1.312	1.58	1.51
H^- in the anion-only lattice						
293 K	0.67	1.770	1.41	1.155	1.73	1.62
160 K	0.68	1.754	1.42	1.165	1.75	1.62
93 K	0.69	1.755	1.39	1.140	1.71	1.62
Li^+ in ^{7}LiD						
293 K	0.28	4.910	0.89	0.776	2.14	0.73
160 K	0.25	5.056	0.88	0.742	2.14	0.72
83 K	0.24	5.170	0.86	0.740	2.12	0.72
D^- in ^{7}LiD						
293 K	0.70	1.651	1.17	1.430	1.38	1.52
160 K	0.69	1.660	1.17	1.435	1.39	1.52
83 K	0.69	1.662	1.18	1.425	1.40	1.52
D^- in the anion-only lattice						
293 K	0.69	1.653	1.28	1.340	1.52	1.61
160 K	0.68	1.660	1.28	1.348	1.52	1.61
83 K	0.69	1.662	1.28	1.340	1.53	1.60

arrangement of electrons at around the same radial distance where the spherical radial density is most strongly reduced.

The resulting effect on the charge density can be discussed on the basis of the angular behaviour of the cubic harmonics $K_n(\theta, \varphi)$, cf. Kurki-Suonio & Sälke (1984). K_4 and K_8 have their main maxima, $K_4 = K_8 = 1$, at the $\langle 100 \rangle$ directions. The maxima of K_4 are surrounded by almost circular zero contour lines with an angular radius of about $30°$, and they have the integral values $\int_{peak} K_4 \, d\Omega = 0.383$. The negative values cover a uniform area and peak to $K_4 = -\frac{2}{3}, \int_{peak} K_4 \, d\Omega = -0.290$ at the $\langle 111 \rangle$ directions. The maxima of K_8 are much sharper with surrounding zero contour lines at about $16°$ angular distance and with the integral values $\int_{peak} K_8 \, d\Omega = 0.108$. Each is surrounded by a negative region with four subsidiary $\langle hhl \rangle$ minima with $K_8 = -0.604$, $\int_{peak} K_8 \, d\Omega = 0.074$ at an angular distance of $27.8°$. In addition there is a uniform positive area with maxima $K_8 = \frac{9}{16}$ and $K_8 = 0.296$ at the $\langle 110 \rangle$ and $\langle 111 \rangle$ directions, respectively. K_6 has its main maxima $K_6 = 1, \int_{peak} K_6 \, d\Omega = 0.198$ in the $\langle 111 \rangle$ directions, strong minima $K_6 = -0.914$, $\int_{peak} K_6 \, d\Omega = -0.185$ in the $\langle 110 \rangle$ directions plus subsidiary maxima $K_6 = \frac{9}{16}$, $\int_{peak} K_6 \, d\Omega = 0.106$ in the $\langle 100 \rangle$ directions.

In H^- all three components accumulate charge in the $\langle 100 \rangle$ directions. K_4 here has the main role, while K_8 mainly causes a tighter concentration. Around the $\langle 110 \rangle$ directions the effects of the sixth and the eighth order largely cancel each other leaving the space between the neighbouring anions empty, and around $\langle 111 \rangle$ there is a vague positive net effect from the three components.

In D^- all nonspherical components are clearly weaker and the sign of the sixth-order component is inverted. As a result, the concentration of charge
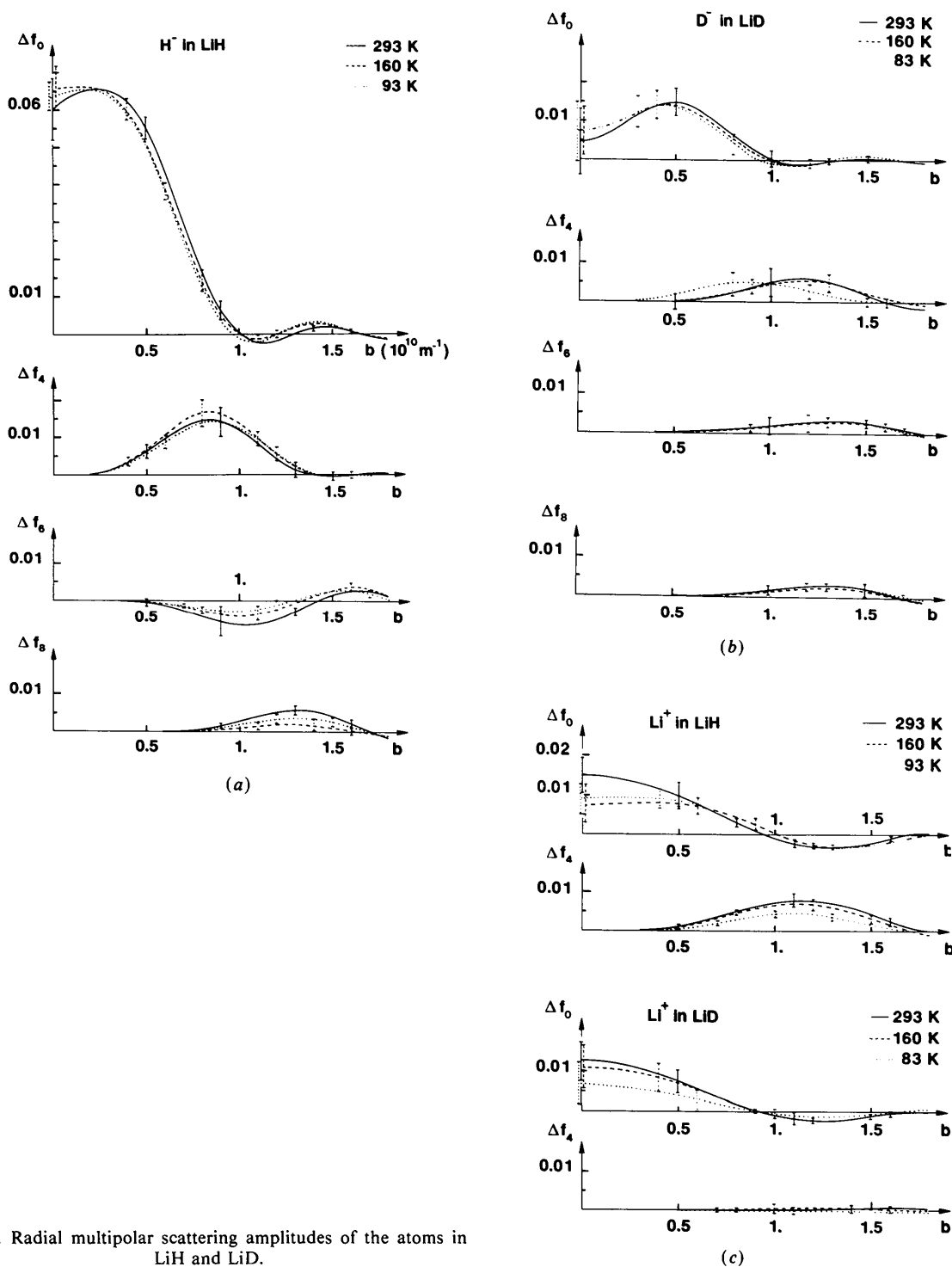
Fig. 2. Radial multipolar scattering amplitudes of the atoms in
LiH and LiD.

density around the ⟨100⟩ directions, as well as the absence of it between the ⟨110⟩ neighbours, is much less marked.

There is some indication of temperature dependence in the sixth- and eighth-order radial atomic factors of H^- in LiH, Fig. 5(a). Its significance is not obvious on the basis of the error bars. However, in terms of electron counts, Fig. 6(a), the strength of the eighth-order component is as much as halved at the lowest temperature compared with the higher temperatures. This would indicate that the concentration of charge density around the ⟨100⟩ directions is somewhat relaxed at low temperatures.

The concentration of charge density around the ⟨100⟩ directions is obviously also the reason for the spurious fourth-order components in the Li^+ SVP atomic factor in LiH. It can be noted that the excess of 0.14e within the SVP sphere exists already in the reference model due to the strong overlapping of the neighbouring anions. The average spherical
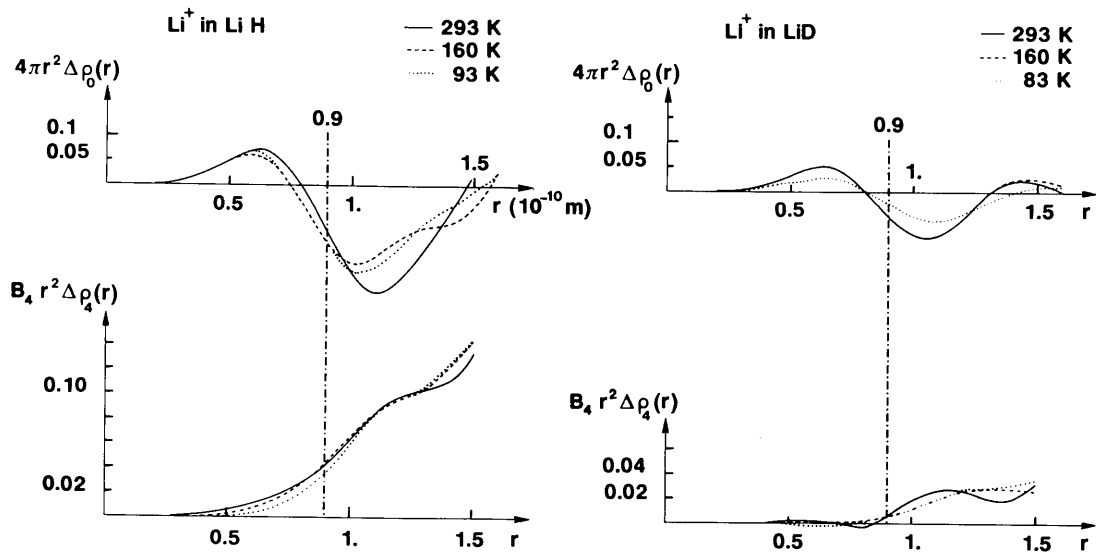
Fig. 3. The multipolar radial densities of Li^+ in LiH and LiD.
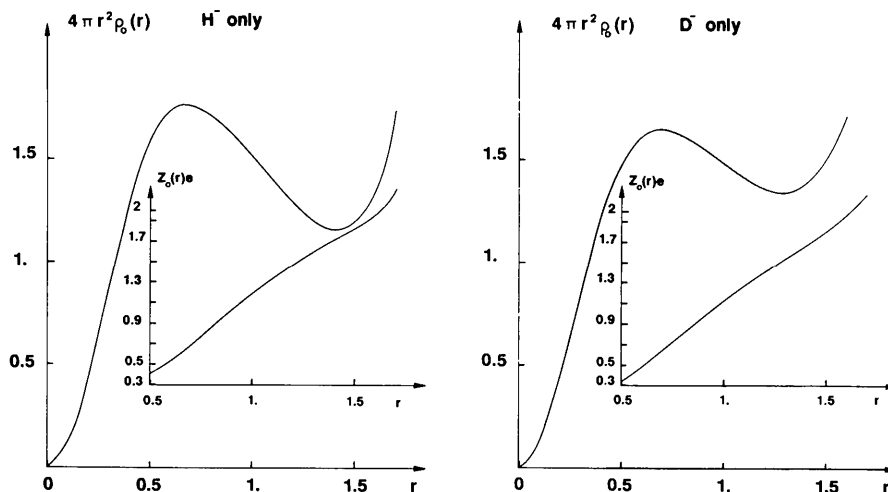
Fig. 4. Radial charge densities around the atomic positions in the anion-only lattices.

compression of the anion, as compared to the model, reduces the overlap density while the angular rearrangement builds it up again. While the net effect, the resulting experimental correction to the electron count, is numerically minute, this state of affairs changes the nature of the extra charge density within and around the lithium area from the trivial geometric overlap effect of the model into a consistent part of the integral angular behaviour of the hydrogen, *i.e.* into some kind of bonding effect involving the electrons of the hydrogen ion only.

Figs. 7 to 10 visualize these features in difference map representations. The concentration of charge density along the $\langle 001 \rangle$ directions and the empty space between neighbouring anions are quite clear in the LiH maps and visible though less evident in the LiD maps. Comparison of the multipolar maps with the conventional Fourier maps shows that these features are due to the consistent three-dimensional behaviour of the anions and should therefore be assigned solely to them.

The phenomenological picture of LiH thus created is such that there is some kind of bonding in the $\langle 100 \rangle$ directions in addition to the ionic Li^+H^- bonding. This extra bonding seems to be between the hydrogen atoms with the Li^+ ion embedded in the middle. In
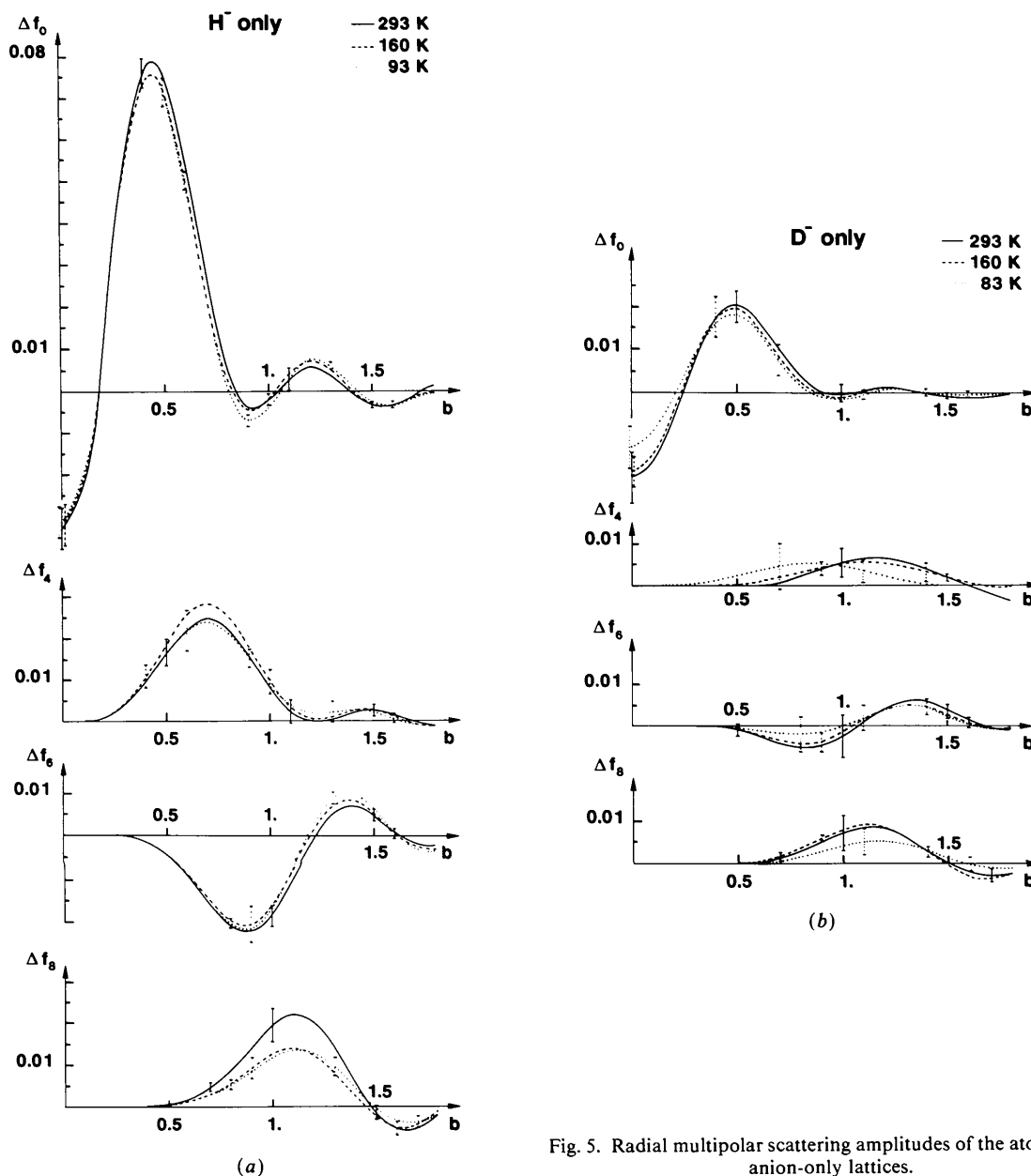
Fig. 5. Radial multipolar scattering amplitudes of the atoms in the anion-only lattices.

any case it is clear from the results that between the neighbouring H^- ions in the $\langle 110 \rangle$ directions there is no bond formation but rather a Pauli repulsion. Recent measurements by Loupias & Chomilier (1986), Mergy (1988) and Loupias & Garreau (1989) of directional Compton profiles of LiH at room temperature seem to support our observations on the bonding charge density. In particular, the differences between the $\langle 110 \rangle$ and $\langle 100 \rangle$ profiles indicate similarly repulsion of the neighbouring $\langle 110 \rangle$ H^- ions and occurrence of bonding charge in the $\langle 100 \rangle$ directions.

When the integral values of the $\langle 100 \rangle$ peaks of the cubic harmonics and the electron counts of the radial densities are taken into account, the rough estimate $0.012e$ per H^- atom and per bond is obtained for the number of electrons participating in the bonding. This is $0.024e$ per bond or $0.071e$ per atom, i.e. 1.8% of all electrons.

It seems that similar but much weaker effects may exist in LiD.

The large difference between the charge distributions of H^- and D^- in itself is an indication of the violation of the Born–Oppenheimer approximation in these crystals. The electronic bonding state depends on the dynamics of the lattice. In particular, the occurrence of the much stronger $\langle 100 \rangle$ bonding in LiH than in LiD reflects the nature and strength of this electron–phonon coupling. One might also speculate that the bonding in LiH and LiD, in addition to the involvement of some electron–phonon coupling, is affected by some resonance effect which strongly favours the hydrogen mass to the deuteron mass.

This coupling seems to be rather independent of temperature in the studied temperature range. There is just a slight indication of weakening at the lowest temperature.
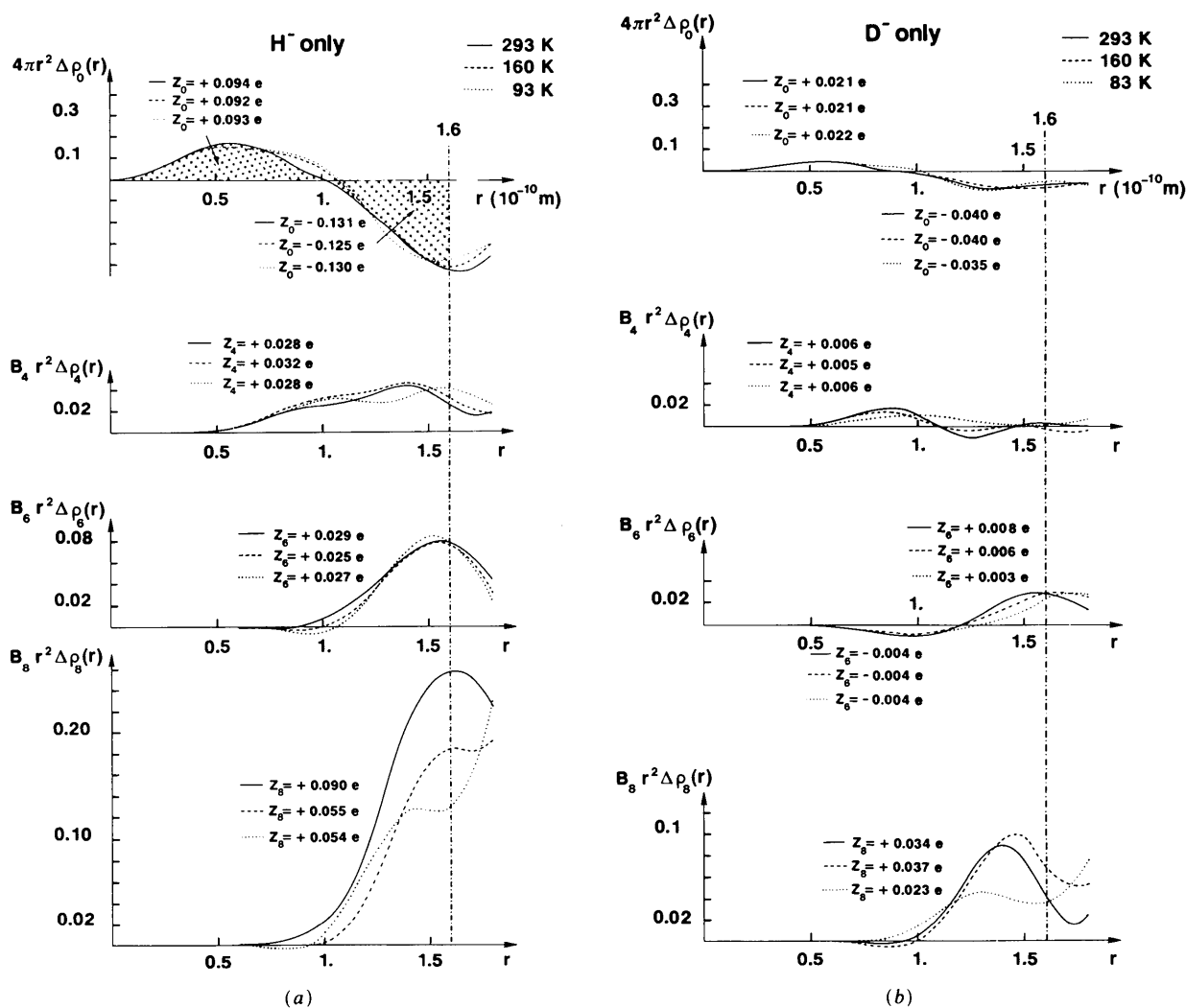
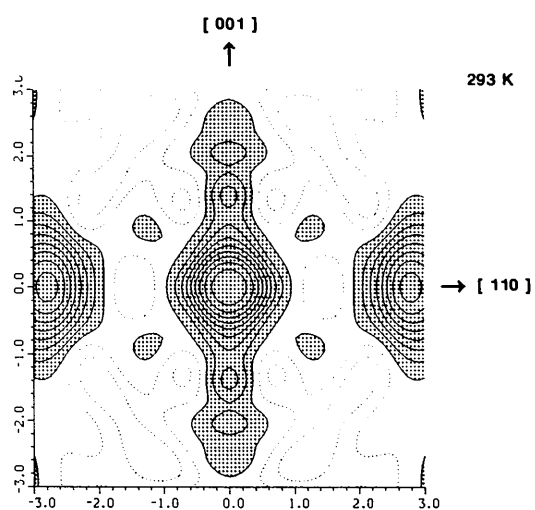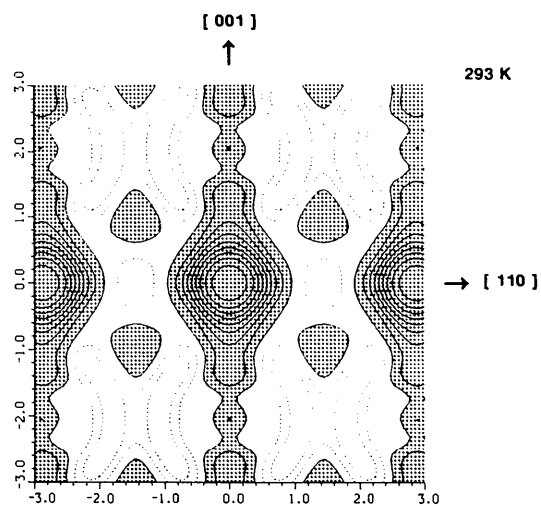Fig. 6. The multipolar radial densities of the atoms in the anion-only lattices.
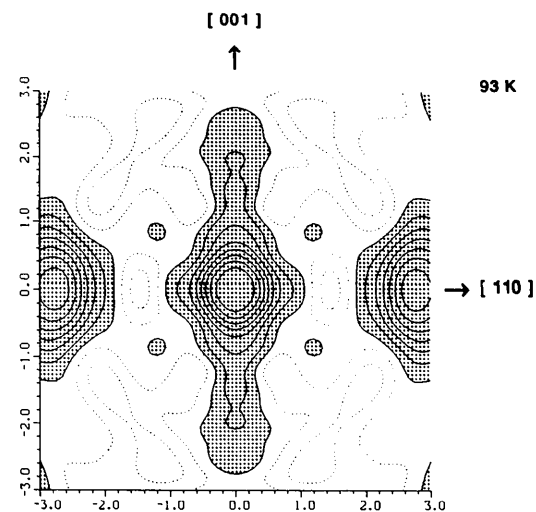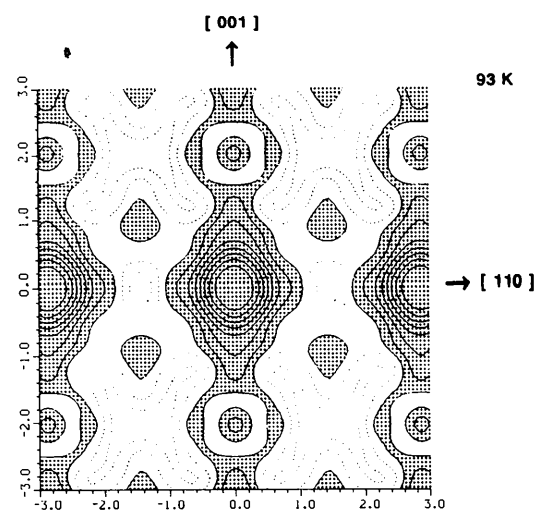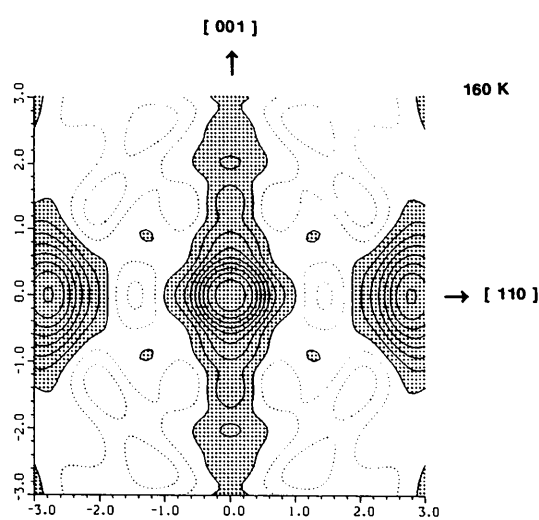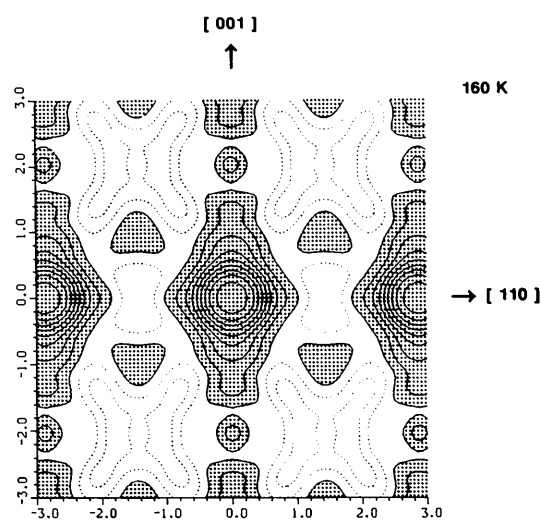
Fig. 7. Difference density of the H$^-$-only lattice in the [110]-[001] plane. Contour interval 0.01×10^{30} e m^{-3}, the regions of positive difference density are shadowed.

Fig. 8. Map of the multipole expansion of the difference density around H$^-$ in the [110]-[001] plane. Contour interval 0.01×10^{30} e m^{-3}, the regions of positive difference are shadowed.
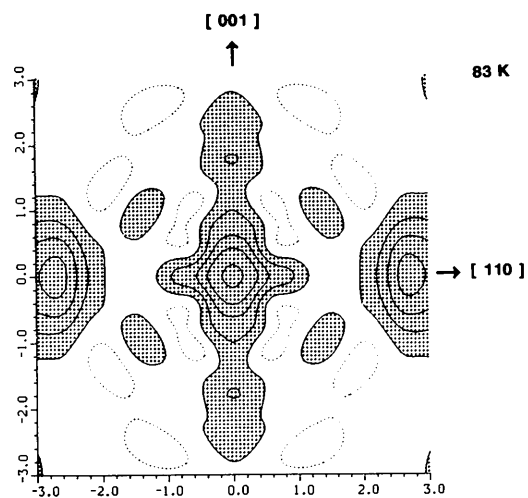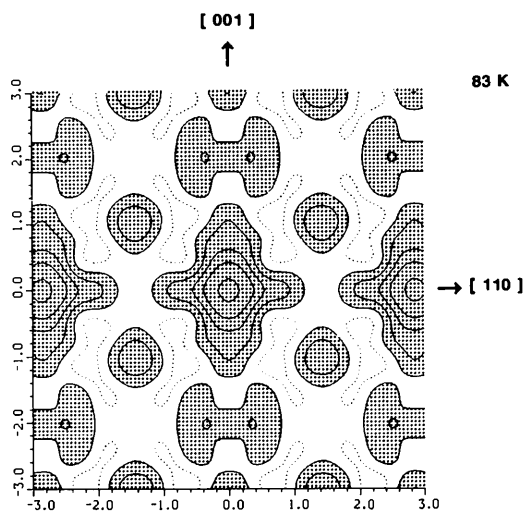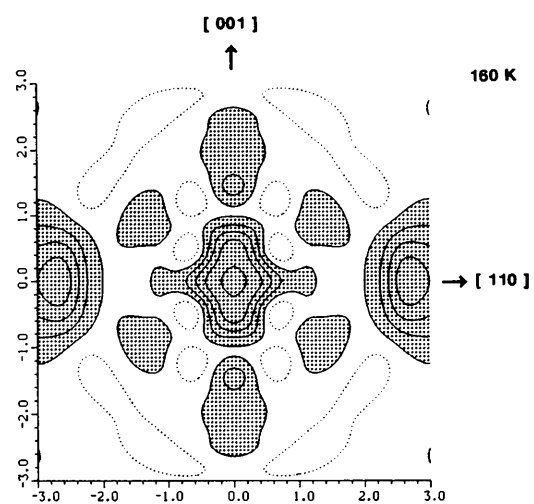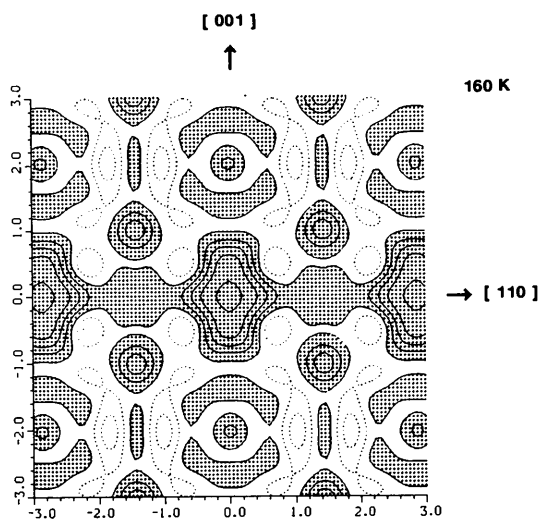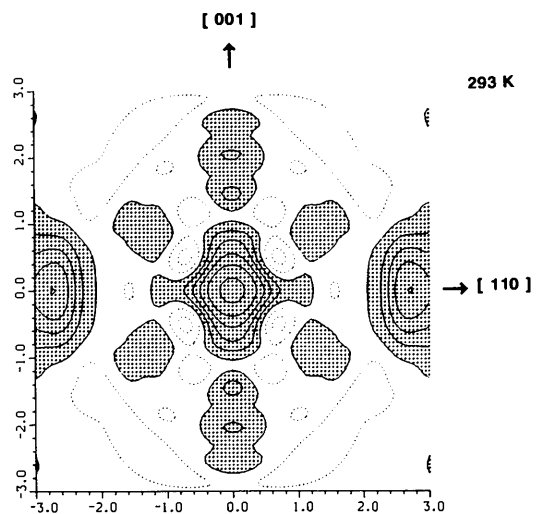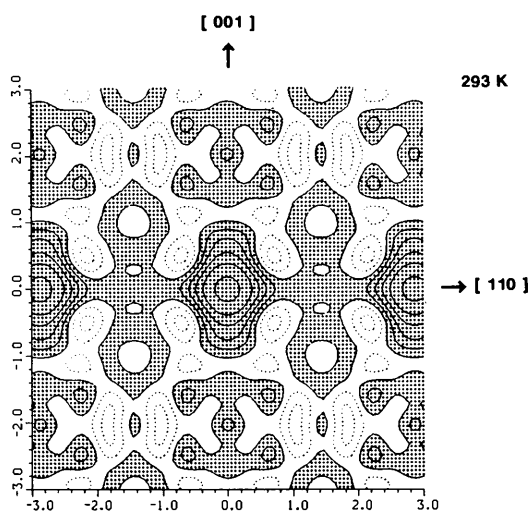
Fig. 9. Difference density of the D⁻-only lattice in the [110]-[001] plane. Contour interval 0.005×10^{30} e m^{-3}, the regions of positive difference are shadowed.

Fig. 10. Map of the multipole expansion of the difference density around D⁻ in the [110]-[001] plane. Contour interval 0.005×10^{30} e m^{-3}, the regions of positive difference are shadowed.

References

ANDERSON, A. & LÜTY, F. (1983). *Phys. Rev. B*, **28**, 3415-3421.
BECKER, P. J. & COPPENS, P. (1975). *Acta Cryst.* A31, 417-425.
BRIEGER, M., RENN, A., SODIEK, A. & HESE, A. (1983). *Chem. Phys.* **75**, 1-9.
CALDER, R. S., COCHRAN, W., GRIFFITHS, D. & LOWDE, R. D. (1962). *J. Phys. Chem. Solids*, **23**, 621-632.
CHAN, Y. C., HARDING, D. R., STWALLEY, W. C. & VIDAL, C. R. (1986). *J. Chem. Phys.* **85**, 2436-2444.
GROSSO, G., PASTORI PARAVICINI, G. & RESTA, R. (1976). *Phys. Status Solidi B*, **73**, 371-378.
HURST, R. P. (1959). *Phys. Rev.* **114**, 3, 746-751.
HURST, R. P., MILLER, J. & MATSEN, F. A. (1958). *Acta Cryst.* **11**, 320-322.
International Tables for X-ray Crystallography (1974). Vol. IV. Birmingham: Kynoch Press. (Present distributor Kluwer Academic Publishers, Dordrecht.)
KARA, M. & KURKI-SUONIO, K. (1981). *Acta Cryst.* A**37**, 201-210.
KURKI-SUONIO, K. & SÄLKE, R. (1984). *Local Density Approximations in Quantum Chemistry and Solid State Physics*, edited

by J. P. DAHL & J. AVERY, pp. 713-733. New York and London: Plenum Press.
KURKI-SUONIO, K. & SÄLKE, R. (1986). *Sov. Phys. Crystallogr.* **31**, 458-461. Engl. transl: American Institute of Physics (1987).
LIU, D. R. (1987). *Solid State Commun.* **63**, 489-493.
LOUPIAS, G. & CHOMILIER, J. (1986). *Z. Phys.* D2, 297-308.
LOUPIAS, G. & GARREAU, Y. (1989). *2nd European Conference on Progress in X-ray Synchrotron Radiation Research. Nuovo Cimento*, **25**, 207-210.
MERGY, J. (1988). Internal Report. Ecole Polytechnique, Paris, France.
PLUMMER, G. M., HERBST, E. & DE LUCIA, F. C. (1984). *J. Chem. Phys.* **81**, 11, 4893-4897.
RAO, B. K. & JENA, K. (1986). *J. Phys. C*, **19**, 5167-5172.
RODRIGUEZ, C. O. & KUNC, K. (1987). *Solid State Commun.* **64**, 19-22.
RODRIGUEZ, C. O. & KUNC, K. (1989). *J. Phys. Condens. Matter*, **1**, 1601-1612.
SÄLKE, R. & KURKI-SUONIO, K. (1984). Report Series in Physics, HU-P-233. Univ. of Helsinki, Finland.
VIDAL, J.-P. & VIDAL-VALAT, G. (1986). *Acta Cryst.* B42, 131-137.
VIDAL, J.-P., VIDAL-VALAT, G., GALTIER, M. & KURKI-SUONIO, K. (1981). *Acta Cryst.* A37, 826-837.
VIDAL, J.-P., VIDAL-VALAT, G. & ZEYEN, C. M. E. (1985). *Nucl. Instrum. Methods*, **228**, 569-575.
VIDAL-VALAT, G., VIDAL, J.-P. & KURKI-SUONIO, K. (1978). *Acta Cryst.* A34, 594-602.

The Distribution of Point Charges on the Surface of a Sphere

BY J. R. EDMUNDSON

Photosol Ltd, Bakers Court, Basildon, Essex SS14 3EH, England

Abstract

The potential, symmetry and Foppl arrangement are given for distributing up to 60 point charges on the surface of a sphere so that the Coulombic potential is a minimum. Some new configurations are described and a general comparison made with the hard-sphere case.

Introduction

The minimization of the potential of N points of unit charge on the surface of a unit sphere can be expressed as

$$V(N, m) = \tfrac{1}{2} \sum_{\substack{i,j=1 \\ i \neq j}}^{N} d_{ij}^{-m}$$

where V is the potential energy, d_{ij} is the distance between points i and j, N is the number of point charges and m is a positive number. When $m = 1$ the Coulombic potential is determined and is known as

Thomson's problem. Tammes's problem is where m approaches infinity. These extreme cases are also known as the soft- and hard-sphere cases respectively and are but two of many similar problems that have been posed over the years. For a more detailed account of these other problems see Melnyk, Knop & Smith (1977) and Ashby & Brittin (1986).

Method of calculation

The technique used to calculate the minimum potential was based on the method described by Metropolis, Rosenbluth, Rosenbluth, Teller & Teller (1953) and Kirkpatrick, Gellat & Vecchi (1986) now known as simulated annealing and exemplified by Wille (1986). Each point is examined together with a number of exploratory positions which form a circle around the point. The angle this circle subtends at the centre of the sphere is denoted as θ. The potential is calculated for these exploratory points; if a lower potential is found then the point charge is moved to